Critical behavior of the banded-unbanded spherulite transition in a mixture of ethylene carbonate with polyacrylonitrile

Bram Sadlik,* Laurent Talon, Sébastien Kawka, Russell Woods, and John Bechhoefer†
Department of Physics, Simon Fraser University, Burnaby, British Columbia, V5A 1S6, Canada
(Received 5 March 2005; published 21 June 2005)

We investigate the transition from unbanded to banded spherulitic growth in mixtures of ethylene carbonate with polyacrylonitrile. By carefully considering systematic errors, we show that the band spacing diverges with a power-law form showing scaling over nearly two decades. We also observe that the bands disorder as the transition point is approached. The critical exponent is nonclassical. One possible explanation is that the nonequilibrium transition is actually weakly first order (subcritical).

DOI: 10.1103/PhysRevE.71.061602 PACS number(s): 81.10.Fq, 81.30.Fb

I. INTRODUCTION

Banded spherulites are commonly seen in solids that freeze from viscous fluids. They comprise one of a number of different "spherulitic" growth modes [1–3], which are characterized by largely radial needle crystals that freeze outward from a central nucleation site as spheres in three dimensions and disks in two dimensions. In addition to being of fundamental interest, spherulites affect the toughness, corrosion resistance, and fracture properties of materials. For example, "nodular" cast iron, where carbon precipitates from the iron matrix as spherulites, is much tougher and more ductile than "gray" cast iron, where the carbon precipitates as graphite flakes [4]. On the other hand, spherulites are a "failure mode" for protein crystallization, since the polycrystalline, radially oriented crystallites cannot be used to provide structural information [5].

Periodic banding in spherulites is associated with a helical twisting of crystalline axes about the radial direction. Such growth is observed in a wide variety of material systems. The majority of studies are of polymer melts [1,3], but there are also observations in liquid crystals [6–8], selenium [9], and low-molecular-weight organics immersed in viscous media (often created by adding polymers [10] or by freezing in gels [2]). Banding occurs in quartz-crystal fibers [11] and hence is important when strongly undercooled, molten rock containing silicates freezes, as in lava flows [12]. Agates are a particularly well-studied example [13,14].

That such similar phenomena are so widely observed suggests a common mechanism; yet the theories that have been proposed all seem to depend on features quite specific to individual systems, and there is no general agreement even about which physical mechanisms are most relevant. It is clear that in banded spherulites, freezing affects the structure of the solid itself. By contrast, at moderate undercoolings and in less-viscous fluids, nearly perfect single crystals are formed, even if morphological instabilities lead to complicated interface shapes (dendrites, snowflakes, etc.) [15].

Broadly speaking, three scenarios for the origins of bands have been advanced. All are at least 40 years old, and none has been universally accepted.

(i)*Screw dislocations*. Eshelby [16] noted that screw dislocations impose an elastic twist on an object. Based on this idea, Schultz and Kinloch [17] proposed that arrays of giant isochiral screw dislocations can lead to a macroscopic twist of crystalline axes. But while there are many observations of screw dislocations associated with banding twist [3], recent atomic force microscope (AFM) observations of the freezing of individual crystallites show that screw dislocations nucleate *after* twisting [18]. At least in the particular system studied, screw dislocations would thus be caused by the twist, and not the reverse.

(ii) *Surface stresses*. Various authors have proposed that surface stresses applied on the crystallite produce forces that are large enough to produce the required elastic twist. Owen has recently given a simple argument predicting the band spacing in such a case [19]. There is substantial disagreement as to the origin of the surface stresses. Keith and Padden have emphasized the role of asymmetry at the end of the growing lamellae, which can produce asymmetric packing of chain folds on the top and bottom of a growing lamellae [20–22]. Patel and Bassett argue the reverse: that asymmetric stresses arise from spontaneous chain reorientation that occurs during the thickening of lamellae well behind the leading edge of the growth [3,23].

(iii) *Diffusion fields*. Keith and Padden proposed that spherulitic growth was connected to diffusion fields that arise during segregation of impurities into the melt [24]. While their original picture is no longer accepted, a variation has recently been set forth by Schultz [25]. He argues that crystals may twist in order to reach areas of lower concentration of some growth-limiting diffusion field. Schultz speculates that this field need not be a concentration of impurities but could also be local stresses generated, for example, by the density difference between solid and liquid. This last suggestion recalls an idea of Tiller and Geering, who used hydrodynamic flows generated by the solid-liquid density difference to account for the splay of spherulites [26,27]. In a recent article, Duan *et al*. give evidence that in very thin polymer films, depletion of the melt in front of the growing film plays a key role in the banding [28].

*Present address: Capilano College, 2055 Purcell Way, N. Vancouver, BC V7J 3H5, Canada.
†Electronic address: johnb@sfu.ca

A number of authors, including Magill [2] and Hutter and Bechhoefer [8], have emphasized that no single theory seems compatible with observations over the full range of systems showing banding (polymers, low- molecular-weight organics, liquid crystals, silicates, etc.) Perhaps different mechanisms are at work in each case, but then why are the macroscopic phenomena so similar?

Faced with these diverging theoretical views on the origins of spherulitic banding, we would like to expand the kinds of experimental measurements available, in order to better constrain the theoretical possibilities. In this article, we explore banded spherulitic growth in a low-molecular-weight material, ethylene carbonate (EC), doped with a small amount of polyacrylonitrile (PAN). To our knowledge, this is the first report of spherulitic growth modes in this system. We focus on the transition from unbanded to banded growth, which occurs as the undercooling ΔT is increased. Here, $\Delta T = T_0 - T$, where T_0 is the solid-liquid coexistence temperature and T is the temperature at the growth front, which may differ from that imposed at the boundaries of the sample. After accounting for a number of systematic experimental effects, we show that at a critical, finite undercooling ΔT_c, the wavelength of the band spacing diverges, with a power law whose exponent is roughly 1. While many previous studies have noted that the band spacing becomes large, there have been no reported measurements of scaling behavior over the wide range of undercooling (two decades) reported here. We discuss possible interpretations of this result.

II. EXPERIMENT

In order to obtain reliable bandspacing measurements at different temperatures, we needed to take considerable care in the experiment. For full details of the apparatus, see the M.Sc. thesis of Sadlik [29]. Briefly, the challenges were to ensure (a) *chemical stability*, since the chemical system showed drifts; (b) *accurate undercooling measurements*, since the release of latent heat changes the temperature at the moving solid-liquid interface; (c) *accurate band spacing measurements*, since the bands show considerable disorder near the transition from unbanded to banded growth

Below, we consider each of these in turn, but first we comment on our choice of system. In a previous report, we explored banded spherulitic growth in a mixture of a low-molecular-weight material (maleic anhydride, MA) with a polymer (polyacrylonitrile, PAN) [10]. The MA-PAN system produces spherulites with exceptionally large bands ($\sim$cm) when frozen at large velocities ($\sim$cm/sec) [30,31], and we wanted to see to what extent the spherulitic growth modes resembled those of other systems with much smaller bands (in polymers, spacings of $1-100$ μm are typical). Unfortunately, the PAN demixes from the host MA material at the undercoolings required to produce bands. Thus, the process of phase separation competes with that of solidification, making the interpretation much more difficult. The present system, EC-PAN, resembles the previous one but the PAN is soluble over a much wider range of temperatures and concentrations. Indeed, EC is a small organic molecule that is typically used as a solvent for hydrophobic polymers, in addition to finding wide industrial use as an ingredient of the liquid electrolytes in lithium-ion batteries [32]. (See the Appendix for material properties.) The bands are still significantly larger than normal polymer systems (up to mm). The slightly smaller band scales simplifies the sample preparation and reduces the effects of latent heat on the undercooling. As we shall see below, one needs to model the latent-heat release to know accurately the undercooling.

We used EC (99.98% pure), as received from the supplier (Huntsman Scientific, 500 Huntsman Way, Salt Lake City, UT). For the PAN, samples of 102-kD chains were used as received from the supplier (Scientific Polymer, 6265 Dean Pkwy, Ontario, NY). We did not observe bands with PAN concentrations $c < 2.6\%$ and could not dissolve the PAN for $c > 7\%$. We thus prepared samples between these limits. (All concentrations are weight %.) To prepare a mixture, we melted an aliquot of pure EC at a temperature of 40 °C. We ground the PAN into a powder and added it to the EC. The mixture was kept at 40 °C and stirred for $1-10$ h, with longer times required for higher polymer concentrations.

A. Chemical stability

Because ethylene carbonate has a high vapor pressure and because it also absorbs water vapor, we needed to find a way to seal samples and assess systematically their drifts and nonuniformity. In order to accomplish this, we built an automated solidification apparatus that could carry out repeated melting and freezing runs. The trickiest task was to automate the nucleation of the solid phase.

The sample was made by sandwiching a thin layer of EC-PAN between a thick copper plate and a glass plate (Fig. 1). The plate spacing was nominally set by two wires (25 μm thick) and the actual average sample thickness d measured by pipetting a known volume of EC-PAN mixture onto the copper plate and measuring the area of the mixture after placing the glass on top. The errors in measuring d were about 5%, and the typical width of the sample was about 4 cm. The samples were sealed with vacuum grease (Dow Corning).

The nucleation method, an automated version of the method of Schaeffer *et al.* [33], is illustrated in Fig. 1. The sample holder is connected to a capillary tube made from a syringe needle, and both are filled with liquid EC-PAN. The end of the tube that is farthest from the sample is frozen and sealed off with a rubber stopper. The bottom end of the tube is held above the coexistence temperature T_0 by means of a small heating coil. The heated region prevents the solid from growing down the tube. To nucleate, one cuts the power to the heating coil, allowing the solid to freeze down into the main sample chamber. Every step is controlled by a visual feedback loop, where a charge-coupled-device (CCD) camera linked by a frame grabber to the control computer verifies that the action (e.g., nucleation) actually took place.

The temperature of the sample is controlled with a commercial regulator [34] containing a Peltier element [35]. The Peltier element is embedded in an aluminum block with a fan and heat sink on the bottom. The copper block of our sample is screwed onto the aluminum block, with paraffin wax be-

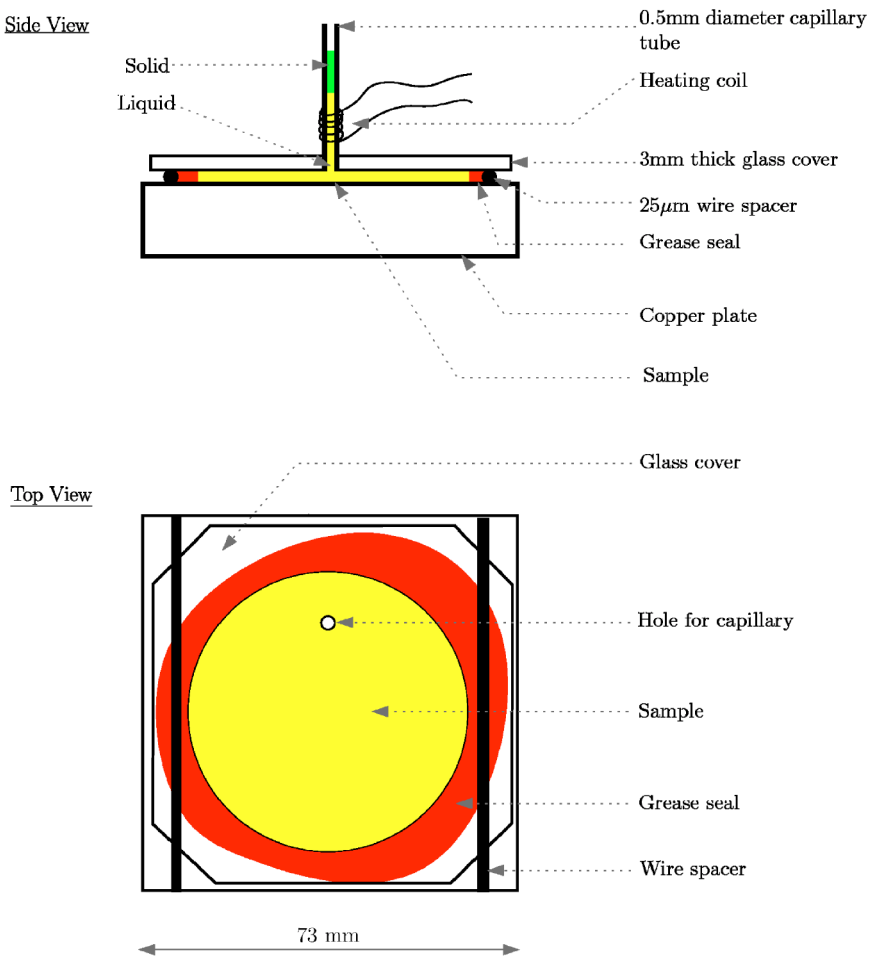

FIG. 1. (Color online). Schematic diagram of sample holder, showing side and top views.

tween to improve thermal contact. The regulator is stable to 1 mK, which far exceeds the experiment's requirements. Temperatures are measured to an accuracy of 0.1 °C by a calibrated thermistor. The sample holder is insulated from the surrounding air by a closed-cell foam box with double-paned glass viewports. The sample was viewed by a CCD camera illuminated off-axis so that specular reflections off the polished, nickel-coated copper plate did not enter the camera's lens.

Preliminary measurements had showed that sample characteristics drift. To assess and reduce drifts, we compared the results of many repeated freezing cycles. This motivated automating the runs. In brief, we created the visual feedback loop mentioned above, monitoring via the CCD camera whether growth had initiated or not. In particular, we could check whether the sample had spontaneously nucleated before reaching the desired undercooling. Without such feedback, it was impossible to obtain the kinds of long, systematic runs needed to track down the sources and magnitudes of the drifts.

The most sensitive monitor of the sample state turned out to be the local front velocity, which is constant but depends on the local temperature and PAN concentration (as well as on impurities resulting from any degradation). To measure the local front velocity, we digitized a movie recording the front growth. Subtracting two successive images removed all but the front, whose intensity profile peak was then fit to a parabola to extract the front position. We then fit the plot of front position versus time to a low-order polynomial whose derivative is our estimate of the velocity.

Typical results are shown in Fig. 2, which show the effects of multiple runs on sealed and unsealed samples. In a long series of runs, we established that the drifts were not due to segregation of PAN or other impurities produced by the solidification process. We also showed that impurities diffuse in from the sample edge and the area around the nucleation site. In a future version of the experiment, one might improve matters by enclosing the sample in an inert atmosphere. Here, we limited the number of runs so that the drifts and nonuniformity in velocity were less than 2%. In practice, we ensured such stability by retaking the first data point at the end of the run.

B. Undercooling measurements

Because a moving interface releases latent heat, no solidification process can be strictly isothermal. For thin films of polymers ($\sim$1 μm) frozen at slow growth rates ($\sim$nm/sec), the temperature rise at the interface is negligible compared to the undercooling. In our case, faster solidification speeds (mm/sec) and a moderate sample thickness (25 μm) imply significant temperature rises (up to 6 °C). Fortunately, for measuring the power law of a critical divergence, knowing that the absolute temperature rise is not necessary. Rather,

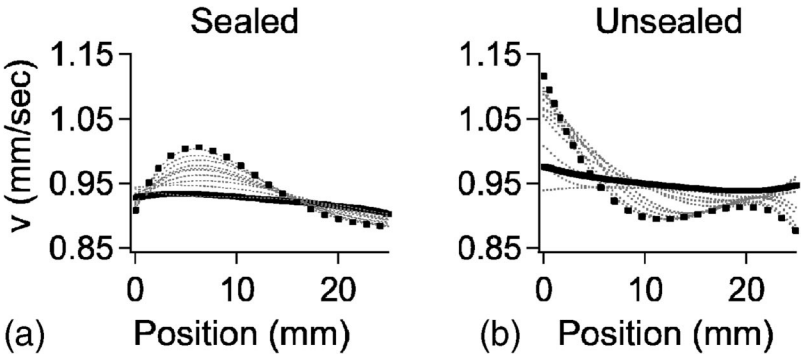

FIG. 2. Front-velocity drifts in EC-PAN samples. Effects of sample inhomogeneities, aging, and sealing can be seen. Thick line: first run. Thin dotted lines: intermediate runs. Thick dotted line: 13th run.

one needs only to estimate the differential correction over the range of undercoolings explored ($\Delta T \leqslant 15$ °C), and even there, only corrections that vary near the divergence undercooling have any effect on the estimate of the critical exponent. While ideally one would measure or calculate the complete temperature field inside the sample, we show by a combination of more simple calculations and experimental measurement that the temperature corrections do not influence our results for the critical exponent.

We begin with the most basic result: Exploring thicknesses ranging from 25 to 75 μm, we observed no change in either the front velocity or band spacing. While this is reassuring, the fact that substantial heating may be expected implies that one should examine this result more closely.

In previous work, we had used an analytical approximation in order to estimate the temperature rise [36]. It is simple to get a rough analytical approximation. The moving front releases a latent heat flux Lv, where L is the molar latent heat and v is the front velocity. The heat must diffuse a distance of the order of the sample thickness d to the copper, which acts as an effective heat sink. The diffusion flux is then roughly $\lambda(\delta T/d)$, where λ is the heat conductivity (nearly the same in both solid and liquid phases) and δT is the typical temperature rise. Equating these fluxes leads to a crude estimate of δT,

$$\delta T \approx \frac{Lvd}{\lambda} = \frac{Lvd}{D\rho C_p} = a\left(\frac{L}{\rho C_p}\right)\left(\frac{vd}{D}\right). \tag{1}$$

In Eq. (1), $L/\rho C_p = 96.3$ °C is the temperature rise produced by the latent heat in the absence of transport away from the transformed material. The term vd/D is the "Peclet number" N_{Pe}, which gives the relative importance of advection and diffusion. We have $v = 1$ mm/s (typically), $d = 25$ μm, and $D_L = 1.00 \times 10^{-7}$ m^2/s, giving $N_{\mathrm{Pe}} \approx 0.25$ and a nominal temperature rise of 24 °C. The dimensionless constant a was evaluated by numerical simulation using finite- element modeling.

The finite-element modeling of heat flow in our experiment was done using commercial software [37]. In the modeling, we took advantage of the ability to use a variable mesh size to simulate the actual geometry of the experiment ($d = 25$ μm thick sample sandwiched between a 7-mm copper block and 2-mm glass plate). We assumed a planar front, since the spherulite radius was several cm, which is much larger than d. We also assumed a vertical interface profile (but see below). Material parameters related to the EC-PAN system may be found in the Appendix. We found that the temperature rise is well described by Eq. (1), with $a = 0.25$. For $d = 25$ μm and $v = 1$ mm/sec, we find $\delta T = 6.1$ °C. Even with $a = 0.25$, Eq. (1) overstates the actual temperature rise, because any deviations of the interface from a vertical profile will reduce the temperature rise still further. In any case, we shall see below that the estimate of the power law for the critical behavior of the band-spacing divergence is extremely insensitive to temperature shifts (i.e., the value of a).

C. Band-spacing measurements

As we shall see, the wavelength λ of the band spacing diverges at a critical undercooling ΔT_c. Near this divergence point, the bands are disordered, and their longitudinal correlation ξ length barely exceeds their wavelength. In this regime, it is difficult to measure the band spacing accurately

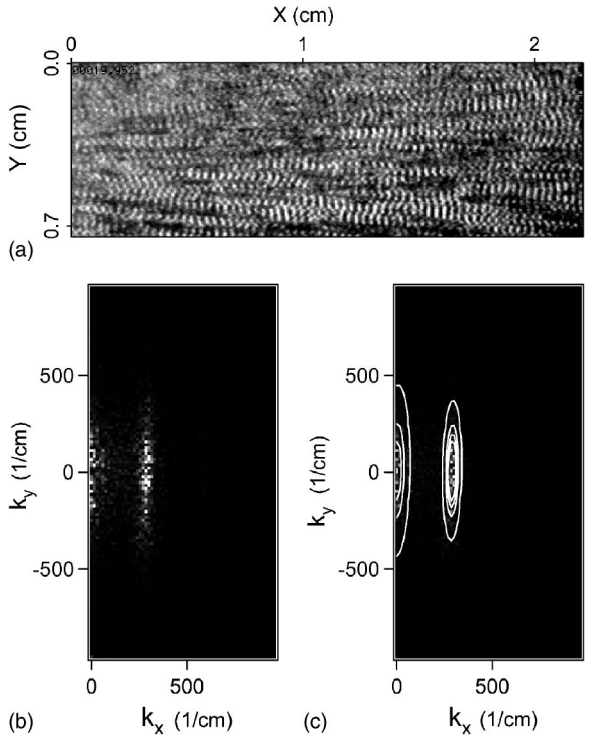

FIG. 3. Banded spherulitic growth in EC-PAN, $c = 6.7\%$. Growth is to the right. (a) Typical image of bands. (b) FFT of image in (a), showing broad peak at the spatial frequency of the bands. (c) FFT with double 2D Gaussian fit superposed on it.

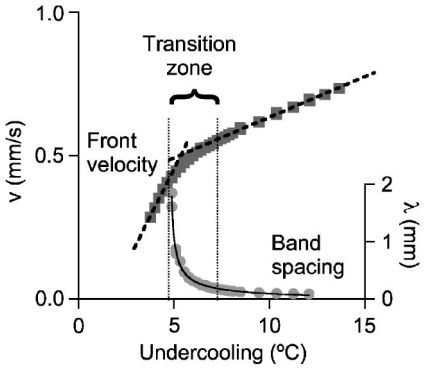

FIG. 4. Front velocity and band spacing versus undercooling for $c=6.7\%$. Dashed lines are straight-line fits to segments of the front-velocity curve and a power-law fit to the band-spacing divergence.

using real-space images. We can average over disorder by analyzing the images in reciprocal space. Figure 3(a) shows a typical image of banded growth. Taking the two-dimensional (2D) Fourier transform of such images [Fig. 3(b)], we find two peaks in k space, one near zero frequency that is due to nonuniformities in illumination and one that represents the periodicity of the pattern. In order to avoid having the zero-frequency peak bias the fit to the other peak, we perform a 2D, double-Gaussian fit to both peaks [Fig. 3(c)]. The band spacing is obtained from the finite-k peak position and the longitudinal correlation is obtained from the peak's width along the x direction. As the wavelength of the bands diverges, the two peaks in the spectrum eventually merge, limiting our ability to measure wavelengths near the critical point. Note finally that we estimated the relative uncertainty in the band spacing (the uncertainty in the estimate of k) by

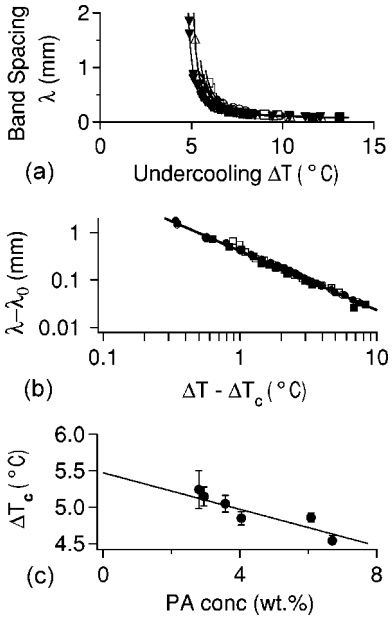

FIG. 5. (a) Band spacing vs undercooling for PAN concentrations of 2.80%, 2.95%, 3.57%, 4.04%, 6.08%, and 6.70%, with global fits shown as solid lines through each data set. (b) Corrected log-log plot of all six data sets. Solid line has a slope of 1.17. (c) Variation of critical undercooling (fits) with concentration.

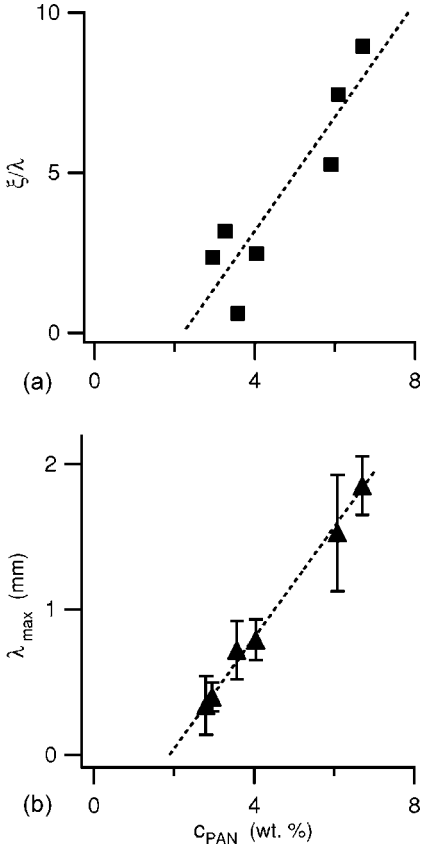

FIG. 6. (a) Scaled longitudinal correlation length vs concentration. (b) Largest observable band spacing vs. concentration.

looking at both the width of the peak in k space, and the statistical uncertainty of the fit. The relative weights of both, as well as those due an examination of run-to-run variation, all follow the same general trend, where the uncertainty in the wavelength increases near the critical divergence point. It was important to account for these increasing errors in the fit for the divergence exponent (Sec. III elow).

III. RESULTS

We measured the front velocity and band spacing in EC-PAN as a function of undercooling for six different concentrations of PAN. A typical result, for a concentration $c=6.7\%$, is shown in Fig. 4. The slope of the velocity-undercooling curve, $dv/d\Delta T$, is different in the banded and unbanded regimes. Interestingly, the slope appears to be correlated with the changing band spacing: it begins to change at the divergence undercooling and essentially stops changing as the band spacing nears its asymptotic value.

Figure 5 are the main results for this paper. Figure 5(a) shows the band spacing versus undercooling for the six concentrations. Because of the divergence of the band spacing and because of the apparently continuous nature of the transition, it is natural to try to analyze the data within the framework of continuous bifurcations. Thus, we fit each curve to a power-law divergence of the form

$$\lambda = \lambda_0 + A(\Delta T - \Delta T_c)^{-\alpha}. \tag{2}$$

We explored various global fits of Eq. (2) to the data where some parameters were local to each curve while others were

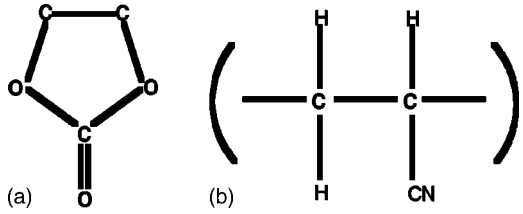

FIG. 7. Chemical structures of (a) ethylene carbonate and (b) polyacrylonitrile.

linked to cover all data sets. If a local fit did not show a systematic variation with concentration, we made the parameter a global one. In the end, λ_0 (intrinsic band spacing), A, and α were all fit globally, while the divergence undercooling ΔT_c was fit locally. Figure 5(b) shows a log-log plot of bandspacing against undercooling with the offsets λ_0 and ΔT_c removed for each data set. The straight line represents a slope of 1.17. Figure 5(c) shows the variation of the individual ΔT_c fit parameters with concentration.

We emphasize that obtaining the results in Fig. 5 requires some care. In particular, it was necessary to control sample-property drifts and to use the proper weights for the errors in the measurement of each λ. Failure to do either of these led to large systematic errors. One systematic error that is harder to estimate is the magnitude of the temperature correction due to latent heat release (Sec. II B). Expressing that correction in terms of the dimensionless factor a defined in Eq. (1), we found that varying a from 0 to 0.25 led to variations in the critical exponent α ranging from 1.22 to 0.95. We thus conclude that $\alpha \approx 1.1 \pm 0.1$, with essentially the entire error due to the uncertainty in the temperature distribution through the cell.

A secondary set of results concerns the regularity of the bands. Figure 6(a) shows the longitudinal correlation length ξ, measured at large undercoolings where there is little temperature dependence, as a function of polymer concentration. The striking trend is that while bands are well ordered at concentrations near 6% (with $\xi \approx 10$ times the band spacing), the ratio of ξ/λ decreases linearly with band spacing, vanishing at about $c=2.8\%$. Figure 6(b) shows a related measurement, the maximum band spacing that could be measured before disorder took over, washing out the bands entirely. That range also decreases linearly with undercooling, vanishing at the same critical polymer concentration.

IV. DISCUSSION

None of the theories of band formation discussed in the Introduction predicts a divergence of band spacing at finite undercooling. It is possible, of course, that more detailed calculations within one of those theories will turn out to make such a prediction. In the meantime, we can consider the generic implications of the wavelength divergence observed at the transition.

The power-law divergence of band spacing [Eq. (2)], along with the increasing effect of fluctuations (Fig. 6), is typical of a second-order morphological transition. We previously noted qualitatively similar behavior in the banded-

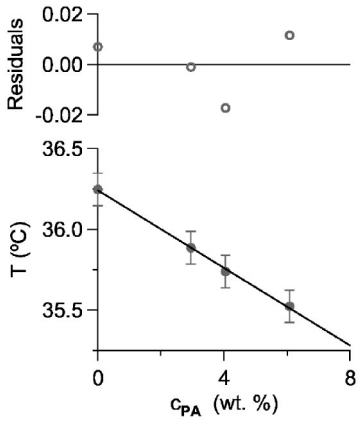

FIG. 8. Liquidus curve for ethylene carbonate with added polyacrylonitrile (102 kD).

unbanded transition of the liquid crystal 10OCB [36,38]; however, in that work, we were unable to obtain data that were accurate enough to fit the form of the divergence. One puzzle, though, is that the value of the critical exponent we obtain is surprising for a second-order transition. We recall several scenarios where patterns show a divergent wavelength at a transition point. Although the scenarios are taken from equilibrium studies, they are all mean-field scenarios. Nonequilibrium, pattern-forming systems (such as growing spherulites) governed by the same dispersion relation (growth rate versus wave number) as one of the scenarios discussed here will show the same wave number scaling with the control parameter [40]. Thus, we view these equilibrium scenarios as possible inspiration for a nonequilibrium theory rather than as being a directly relevant description.

One scenario is the Lifshitz point, where the gradient term in a free-energy expansion changes sign [39]. Such a transition leads to a divergence with exponent $\alpha = 1/2$, a value that is incompatible with our results. A recent study of Chuang *et al.* [41] measured the band spacing versus undercooling at the transition and claims a result compatible with $\alpha = 0.5$. It is possible that different systems show different exponents, of course. But we note that their data, in contrast to the present study, cover a range of less than one decade and show considerable curvature. The authors also do not mention whether they corrected for the kinds of systematic errors discussed here.

A second scenario for a structure with diverging wavelength is the "solitonic" transition [42]. One example is the unwinding of a cholesteric liquid crystal in an external field that aligns molecules along the field [43]. In that scenario, the divergence depends on the nature of the interactions between molecules. In the typical case, the interactions are short range, and the divergence occurs logarithmically—i.e., more slowly than any power law. This is also incompatible with our results. If there are long-range power-law interactions between molecules, the structure spacing will also diverge with a power law. It is unclear what the relevant interactions are here, but we note that because of hydrodynamic coupling, polymers do show long-range interactions in solution, as described by the Oseen tensor [44].

A third scenario is that of a weakly first-order transition, where would-be power-law divergences are interrupted by an

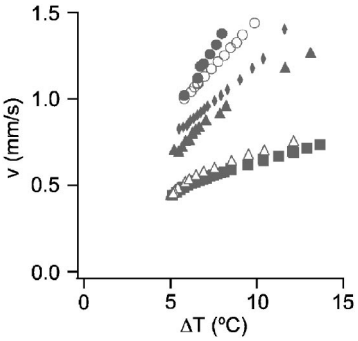

FIG. 9. Solid-liquid front velocity versus undercooling for different PAN concentrations, in the regime showing banding. ●, 2.80 wt. %; ○, 2.95 wt. %; ◆, 3.57 wt. %; ▲, 4.04 wt. %; △, 6.08 wt. %; ■, 6.70 wt. %.

abrupt transition. One such experimental situation that at least superficially resembles the present one is the divergence of the pitch of a cholesteric liquid crystal in the vicinity of a smectic-*A* transition. Symmetry requires that the transition be first order, but in practice the discontinuities are very weak. Huang *et al.* measured power-law divergences in several cholesterics, as the temperature was lowered into the smectic phase. The study that is most relevant to our work here is a study of cholesteryl nonanoate doped with a controlled concentration of cholesteryl chloride [45]. In that work, the critical exponent was found to vary with concentration from 0.67 to 1.15. Vigman and Filev have claimed to explain these results as being due to a first-order transition [46,47]. Their theory at least superficially uses many features specific to the free energy of a cholesteric and of a smectic. It would be interesting to revisit their work in a more general context.

Of the three scenarios, the third seems at present most compatible with our results, but more work is required to judge its plausibility. We note that the variation in the cutoff of λ_{max} with concentration observed in Fig. 6(b) might then be interpreted as a shift in the first-order point of the transition. It would be interesting to see then whether the results on the variation of the correlation length ξ near the transition are also compatible with such a model. To our knowledge, no one has yet calculated ξ in any of these scenarios. Finally, we note again that our system is a nonequilibrium one and that one would have to seek a dynamical model with a weakly subcritical bifurcation.

V. CONCLUSIONS

By carefully controlling various systematic effects, we have measured a power-law divergence of band spacing at the banded-to-unbanded transition of the EC-PAN system. We have considered several scenarios that might generically account for such a divergence (with a nonclassical exponent), of which a weakly first-order scenario at present seems most likely. It would be important to find other systems to test experimentally, to see to what extent the exponent varies. In the weakly first-order scenario, there is not a true power-law divergence. The measured exponent is expected not to be universal and should depend on the system examined. It is also interesting to try to develop the first-order scenario more generically, to better isolate its general features.

At the same time, the observation of critical behavior reported here places a constraint on any theory of the banded-unbanded transition. While many of the features of such a transition will be generic in the sense of being independent of the details of the physics of the scenario, the presence of such a divergence in a theory is by no means automatic. Indeed, none of the possible theories of the banded-unbanded transition discussed in the Introduction has been explored in enough detail to know whether they predict a band spacing divergence or not, let alone what kind of divergence is predicted. We hope that our experiments will motivate a more careful examination of these theoretical possibilities.

ACKNOWLEDGMENTS

This research was supported by NSERC (Canada). Mike Degen made the original discovery that the EC-PAN system

TABLE I. Thermodynamic properties of pure ethylene carbonate.

Formula		$C_3H_4O_3$	
CAS registry number		96-49-1	
Molecular weight		88.06 g mol^{-1}	[48]
Coexistence temperature (solid-liquid)	T_0	36.4 °C	[48]
Density (liquid, 40 °C)	ρ_L	1321.991 kg m^{-3}	[49]
Density (solid, 36 °C)	ρ_S	1470 kg m^{-3}	[50]
Heat capacity (liquid, 36 °C)	$C_{p,L}$	138.0 J mol^{-1} K^{-1}	[48]
Heat capacity (solid, 25 °C)	$C_{p,S}$	117.4 J mol^{-1} K^{-1}	[48]
Thermal conductivity (liquid, 41 °C)	λ_L	0.2063 W m^{-1} K^{-1}	[51]
Thermal diffusivity (liquid)	$\lambda_L(\rho_L C_p, L)$	1.00×10^{-7} m^2 s^{-1}	derived
Latent heat	L	13295 J mol^{-1}	[52]
Undercooling scale	$L/C_{p,L}$	96.3 °C	derived
Crystal structure		monoclinic	[50]
Lattice parameters		a=8.92, b=6.25, c=6.94 Å, β=100.5 °	[50]
Space group		$C2/c$	[50]

shows banded spherulites, and he and Matthew Case did valuable preliminary studies.

APPENDIX: SOME RELEVANT MATERIAL PROPERTIES

Here, we collect some relevant material properties of ethylene carbonate and polyacrylonitrile. Figure 7 shows their chemical structure, Fig. 8 shows the liquidus line of the EC-PAN phase diagram, and Fig. 9 shows front-velocity measurements as a function of undercooling. These measurements were used to correct the undercooling values. Table I summarizes various thermodynamic properties of EC.

[1] P. J. Phillips, in *Handbook of Crystal Growth*, edited by D. T. J. Hurle (Elsevier, Amsterdam, 1994), Vol. 2, Chap. 18, pp. 1167.
[2] J. H. Magill, J. Mater. Sci. **36**, 3143 (2001).
[3] D. C. Bassett, J. Macromol. Sci., Pure Appl. Chem. **42**, 227 (2003).
[4] W. L. Bradley and M. N. Srinivasan, Int. Mater. Rev. **35**, 129 (1990).
[5] *Crystallization of Nucleic Acids and Proteins: A Practical Approach*, edited by A. Ducruix and R. Giegé (Oxford University Press, Oxford, 1992).
[6] Friedrich Rinne, Trans. Faraday Soc. **29**, 1016 (1933).
[7] S. C. Jain, S. A. Agnihotry, and V. G. Bhide, Mol. Cryst. Liq. Cryst. **88**, 281 (1982).
[8] J. L. Hutter and J. Bechhoefer, J. Cryst. Growth **217**, 332 (2000).
[9] J. Bisault, G. Ryschenkow, and G. Faivre, J. Cryst. Growth **110**, 889 (1991).
[10] M. M. Degen, N. Costanzino, and J. Bechhoefer, J. Cryst. Growth **209**, 953 (2000).
[11] C. Frondel, Am. Mineral. **63**, 17 (1978).
[12] A. D. Fowler, B. Berger, M. Shore, M. I. Jones, and J. Ropchan, Precambrian Res. **115**, 311 (2002).
[13] Y. Wang and E. Merino, Geochim. Cosmochim. Acta **54**, 1627 (1990).
[14] P. J. Heaney and A. M. Davis, Science **269**, 1562 (1995).
[15] *Solids far from Equilibrium*, edited by C. Godrèche (Cambridge, University Press, Cambridge, England, 1992).
[16] J. D. Eshelby, J. Appl. Phys. **24**, 176 (1953).
[17] J. M. Schultz and D. R. Kinloch, Polymer **10**, 271 (1969).
[18] J. Xu, B.-H. Guo, Z.-M. Zhang, J.-J. Zhou, Y. Jiang, S. Yan, L. Li, Q. Wu, G.-Q. Chen, and J. M. Schultz, Macromolecules **37**, 4118 (2004).
[19] J. Owen, Polym. Commun. **38**, 3705 (1997).
[20] H. D. Keith and F. J. Padden, Jr., Polymer **25**, 28 (1984).
[21] H. D. Keith and F. J. Padden, Jr., Macromolecules **29**, 7776 (1996).
[22] H. D. Keith, Polymer **42**, 9987 (2001).
[23] D. Patel and D. C. Bassett, Polymer **43**, 3795 (2002).
[24] H. D. Keith and F. J. Padden, Jr., J. Appl. Phys. **34**, 2409 (1963).
[25] J. M. Schultz, Polymer **44**, 433 (2003).
[26] G. T. Geering, Ph.D. thesis, Stanford University, 1968.
[27] W. A. Tiller, *The Science of Crystallization: Macroscopic Phenomena and Defect Generation* (Cambridge University Press, Cambridge, England, 1991).
[28] Y. Duan, Y. Jiang, S. Jiang, L. Li, S. Yan, and J. M. Schultz, Macromolecules **37**, 9283 (2004).
[29] B. Sadlik, M.Sc. thesis, Simon Fraser University, 2004.
[30] R. R. Lagasse, J. Cryst. Growth **140**, 370 (1994).
[31] B. J. Olivier, R. R. Lagasse, D. W. Schaefer, J. D. Barnes, and G. G. Long, Macromolecules **29**, 8615 (1996).
[32] M. Wakihara, Mater. Sci. Eng., R. **33**, 109 (2001).
[33] R. J. Schaeffer, M. E. Glicksman, and J. D. Ayers, Metall. Trans. A **7**, 1747 (1976).
[34] Wavelength Electronics, 51 Evergreen Dr., Suite B, Bozeman, MT 59715, USA (www.wavelengthelectronics.com), model HTC3000.
[35] Tellurex Co., 1248 Hastings St., Traverse City, MI 49686, USA (www.tellurex.com/), model CA1-1.0-127-1.27 Z-max module.
[36] J. L. Hutter and J. Bechhoefer, Phys. Rev. E **59**, 4342 (1999).
[37] Femlab, v. 3.0a; COMSOL, Inc., 1100 Glendon Avenue, 17th Floor, Los Angeles, CA 90024 USA (www.comsol.com).
[38] J. L. Hutter and J. Bechhoefer, Phys. Rev. Lett. **79**, 4022 (1997).
[39] P. M. Chaikin and T. C. Lubensky, *Principles of Condensed Matter Physics* (Cambridge University Press, Cambridge, England, 1995).
[40] M. Cross and P. Hohenberg, Rev. Mod. Phys. **65**, 851 (1993).
[41] W. T. Chuang, P. D. Hong, and H. H. Chuah, Polymer **45**, 2413 (2004).
[42] R. D. Kamien and J. V. Selinger, J. Phys.: Condens. Matter **13**, R1 (2001).
[43] P. G. de Gennes and J. Prost, *The Physics of Liquid Crystals*, 2nd ed. (Clarendon Press, Oxford, England, 1993).
[44] M. Doi and S. F. Edwards, *The Theory of Polymer Dynamics* (Oxford Science, Oxford, 1986).
[45] C. C. Huang, R. S. Pindak, and J. T. Ho, Phys. Lett. **47A**, 263 (1974).
[46] P. B. Vigman and V. M. Filev, Sov. Phys. JETP **42**, 747 (1976).
[47] S. A. Pikin, *Structural Transformations in Liquid Crystals* (Gordon and Breach, New York, 1991).
[48] NIST Chemistry WebBook (http://webbook.nist.gov).
[49] R. Naejus, D. Lemordant, and R. Coudert, J. Chem. Thermodyn. **29**, 1503 (1997).
[50] C. J. Brown, Acta Crystallogr. **7**, 92 (1954).
[51] C. L. Yaws, *Handbook of Thermal Conductivity* (Gulf Publishing, Houston, 1995), Vol. 1, p. 146.
[52] I. A. Vasil'ev and A. D. Korkhov, Russ. J. Phys. Chem. **47**, 1527 (1973).